A GENERAL MODELLING APPROACH FOR COATED COTTON-SEEDS BASED ON THE DISCRETE ELEMENT METHOD
/
基于多目标优化的包衣棉种离散元接触参数标定

Wang Long[1, 2, 3], Hu Can[1, 2, 3], He Xiaowei[1, 2, 3], Guo Wensong[2, 3], Wang Xufeng[2, 3], Hou Shulin[1*] [1]

[1)] College of Engineering, China Agricultural University, Beijing, 100083 / China;

[2)] College of Mechanical and Electronic Engineering, Tarim University, Alar Xinjiang, 843300 / China;

[3)] Key Laboratory of Colleges & Universities under the Department of Education of Xinjiang Uygur Autonomous Region, Alar Xinjiang 843300/ China

Tel: +86 13581711364; E-mail: hsl010@126.com

DOI: https://doi.org/10.35633/inmateh-63-22

Keywords: *coated cotton seeds; discrete element; parameter calibration; optimal design*

ABSTRACT

In the current paper, a coated cotton-seed discrete element model was established. Furthermore, we designed a device for the simultaneous determination of the repose and accumulation angles, and Plackett–Burman and central composite design (CCD) tests were performed with the repose and accumulation angles as the test indexes. The static friction coefficient between seeds (SFCC) and the dynamic friction coefficient between seeds (DFCC) were observed to have a significant influence on the indexes and were thus selected for the subsequent analysis ($P < 0.05$). Analysis of variance revealed the terms of these two parameters to have a significant effect on the relative error of the repose angle (RERA) and the relative error of accumulation angles (REAA) ($P < 0.05$). A solution to the proposed mathematical model was determined via the NSGA-Ⅱ genetic algorithm and the Pareto optimal solution set was obtained. Based on multi-objective optimization, the SFCC and DFCC were determined as 0.174 and 0.068, for RERA and REAA values of 1.715% and 1.712%, respectively. Simulations were then performed using the optimal parameters. Results of the T-test demonstrated that there were no significant differences between the simulated and physical test results.

摘要

本文基于 EDEM 软件建立了包衣棉种离散元模型，设计了一种可以对物料休止角与堆积角同时进行测定的装置，通过物理试验与仿真试验对棉种接触参数进行了标定。首先，利用 Plackett-Burman 试验筛选出了对棉种休止角和堆积角有显著性影响的接触参数，为种间静摩擦系数和种间动摩擦系数；然后以休止角和堆积角相对误差为指标，对这两个参数进行最陡爬坡试验，优化其取值范围，并基于中心组合试验建立了指标与显著性参数的回归数学模型，数学模型的拟合度较好；进而采用遗传算法(NSGA-Ⅱ)进行多目标寻优，得到当种间静摩擦系数为 0.174，种间动摩擦系数为 0.068 时，棉种离散元模型的数学模型最优解较好；最后利用 T 检验得到休止角和堆积角的 P 值均大于 0.05，表明仿真试验与物理试验值差异不显著，验证了最优参数组合的可靠性。

INTRODUCTION

The rapid development of computer technology has facilitated the application of the discrete element method (DEM) in the study of agricultural bulk material. In particular, DEM can intuitively and quantitatively analyse the force and movement law of agricultural materials (*Liang et al., 2020*). For example, in the application of seed metering devices, DEM is employed to reveal the movement process and mechanisms, as well as to optimize the corresponding parameters and performance (*Gao et al., 2020; Hou et al., 2020*). The northwest region of China has become the principal cotton producing area in China, due to its special natural environment and soil conditions, obviously characterized by an arid climate, low rainfall, evaporation, and temperature difference between day and night, and long hours of sunshine. Existing cotton precision seed metering devices are prone to miss and repeat sowing, requiring farmers to supplement or thin the

[1] *Wang Long, Ph.D. Stud.; Hu Can, Ph.D. Stud.; He Xiaowei, Ph.D. Stud.; Guo Wensong, A. Prof. Ph.D.; Wang Xufeng, Prof. Ph.D.; Hou Shulin, Prof. Ph.D.;*

seedlings following sowing. In order to improve the performance of seed metering devices, several studies have adopted the discrete element method to analyse the mechanisms underlying the seed metering process and to subsequently optimize the structure (*Binelo et al., 2019*). The parameter and model accuracies play a crucial role in these studies. Previous research generally includes three-dimensional models and the characteristic and contact parameters of the material. Thus, it is necessary to reconstruct the material shape and calibrate and optimize the corresponding parameters prior to simulations (*Xue et al., 2019*).

Numerous scholars have performed research on the three-dimensional modelling and parameter calibration of crop seeds. Such work initially requires the establishment of an accurate three-dimensional seed model. This can be determined via three-dimensional software based on the seed shape and size, or reconstructed using reverse engineering technology, with the latter option proving to be more accurate and is thus widely used (*Zhou et al., 2020; Qi et al., 2019*). As the discrete element method is based on spherical particles, the discrete element seed particle model must be determined with spherical particles. The bonded particle and multi-sphere methods are commonly employed to establish discrete element particle models. The more spherical the particles, the closer the model is to the physical structure, irrespective of the method used (*Zhang et al., 2020; Yan et al., 2020*). Once the particle model is established, the parameters need to be calibrated to ensure that the simulation can truly reflect the movement process of the material and the underlying mechanisms, such that it can directly be used in simulation research. Physical and simulation tests are generally combined for the parameter calibration (*Ghodki et al., 2019; Wang et al., 2020*).

The long-term planting of cotton increases the amount of germs in the crop, while low temperatures are critical for seedling emergence. Due to this, cotton seeds in northwest China need to be coated in order to improve the germination and seedling preservation rate and to control bacteria (*Li et al., 2018*). More specifically, a seed coat agent is typically coated on the cotton seed surface. Commonly used seed coat agents include carboxin, thiram and salicylic acid. Such agents alter the surface characteristics of the cotton seeds (*Furuhata et al., 2011*). Simulation errors are typically a function of the accuracy of the model and parameters. The accurate calibration of the cotton seed model and its related parameters can greatly improve the accuracy of simulations (*Liu et al., 2016*).

In the current paper, we design a device to measure the repose and accumulation angles of coated cotton seeds, and establish a discrete element model for coated cotton seeds. A Plackett-Burman design was adopted to identify which contact parameters had a significant influence on the indexes based on the repose and accumulation angles. The steepest ascent and central composite design (CCD) were used to reduce the range of parameters. The regression mathematical model between the contact parameters and the index was then established and a genetic algorithm was employed to optimize the mathematical model, thus obtaining the optimal contact parameters. The optimal contact parameters were then used for simulation testing and the results were compared with the real physical test values to verify the simulations. The results of this paper can provide a reference for future DEM-based research on the material contact parameter settings during the movement process and mechanism of coated cotton seeds using a seed metering device.

MATERIALS AND METHODS

The test materials were selected from Zhongmian-96A coated cotton-seeds produced by Zhongmian Seed Industry in Akesu city, China in 2019. The effective components of the seed coating agent were carboxin and thiram, with a content of 200 g/L used for both agents. The density, 1,000 seed weight and average moisture content of the cotton seeds were 0.9793 g/ml, 88.14 g, and 7.3 % (w.b.), respectively.

A total of 200 cotton seeds with a regular shape were randomly selected, and the three-axis dimension was measured using a digital explicit vernier caliper (BK-318 with a 0.01 mm precision) (Figure 1). The length L, width W and thickness T of the cotton seeds were determined as 9.04±0.48 mm (mean ± standard deviation), 4.66±0.28 mm and 4.06±0.29 mm, respectively. The cotton seed volume V was determined as follows (*Baryeh and Mangope, 2003*):

$$V = \frac{\pi B^2 L^2}{6(2L - B)} \quad (1)$$

where $B=(WT)^{1/2}$, V is the volume of cotton seed (mm^3), L is the length of cotton seed (mm), W is the width of cotton seed (mm), T is the thickness of cotton seed. The volume distribution of cotton seeds is essentially normal, with mean and standard deviation values of 59.15±7.69 mm^3 (Figure 2).

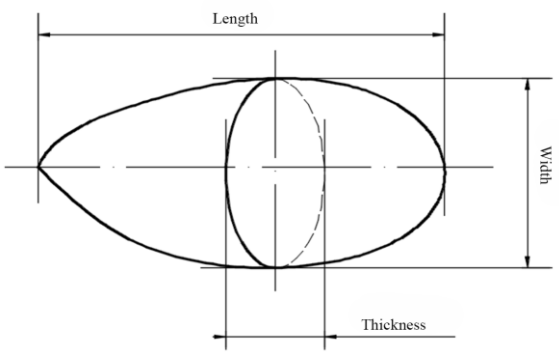

Fig. 1 - Three-dimensional dimension of cotton seed

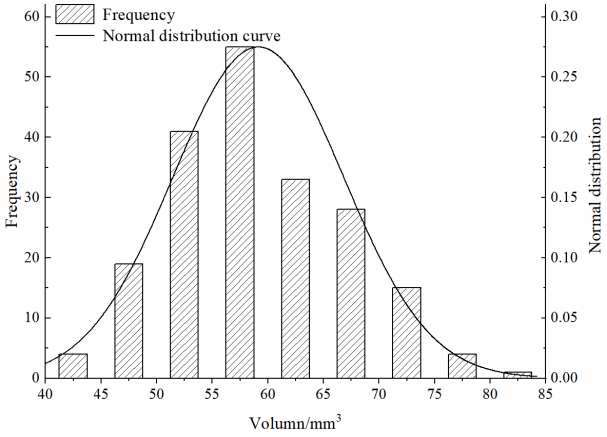

Fig. 2 - Distribution of cotton seed volume

Figure 3 presents the device used for the seed drop testing. The device is made of transparent plexiglass with a Poisson's ratio of 0.5, a density of 1180 kg/m^3, and a shear modulus of 177 MPa (*Han et al., 2018*) and is composed of a seed box, baffle, funnel and disk. The seed storage chamber is of dimensions 150 x 50 x 200 (length x width x height) and the inner diameter and height of the disc are 62 mm and 20 mm, respectively. The testing procedure can be described as follows. The baffle was inserted into the seed box prior to testing. Cotton seeds free from damage and defects were then selected and added into the seed box, filling 3/4 of the box. The upper surface of the seed layer was maintained as close to the horizontal plane as possible. The baffle was then removed, allowing the cotton seeds to slide down the opening, through the funnel and into the disc. Once the cotton population in the seed box and disk was stable, the angle between the inclined and horizontal planes in the seed box and the disk were measured, and denoted as the repose angle β and accumulation angle φ, respectively.

Fig. 3 - Experimental equipment

In order to reduce errors in the artificial measurement process, MATLAB 7.2 (MathWorks) was adopted to process the acquired images (Figure 4) using a median de-noising filter, gray processing and binary processing. The population boundary curve was obtained by extracting the population boundary contour and the least squares method was used to fit the boundary curve. The slope of the straight line was equal to the tangent value of the repose and accumulation angles, and was determined based on the slope of the straight line. The average values and variance of the actual repose angle and angles of the cotton population were determined as 34.70±0.49° and 29.05±0.32°, respectively, following 10 repetitions. The results reveal a significant difference between the repose and accumulation angles (P = 0.552), and thus they can be used as analysis indexes for the subsequent analysis.

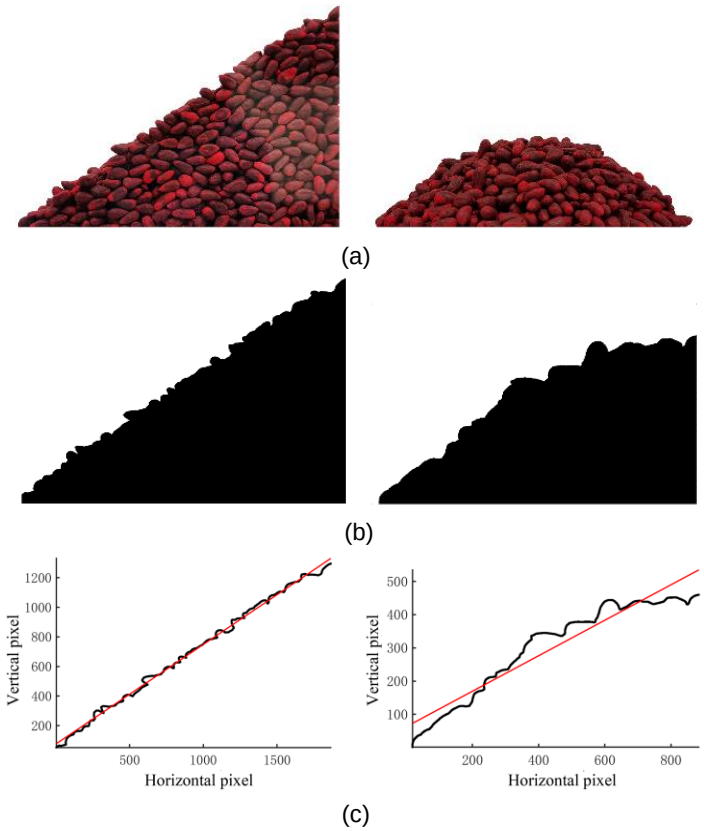

Fig. 4 Image processing of the repose and accumulation angles

(a) image acquisition; (b) binary processing; (c) the contour curve is fitted as a straight line

The Herz-Mindlin contact model was selected for the simulation process. In order to realistically simulate the actual test process, the cotton seed particle model volume was generated according to the normal distribution of the actual cotton seed volume. The cotton seed particle quantities and test process follow those of the physical testing. The total number of cotton seed particles was 5,272, which reached a stable state in the seed box at 0.24 s. The baffle was then removed and the cotton seed particles fell into the disk through the funnel. Following the simulation test, images of the repose and accumulation angles were acquired (Figure 5) and processed in MATLAB to obtain the repose angle β' and accumulation angle φ' of the population simulation.

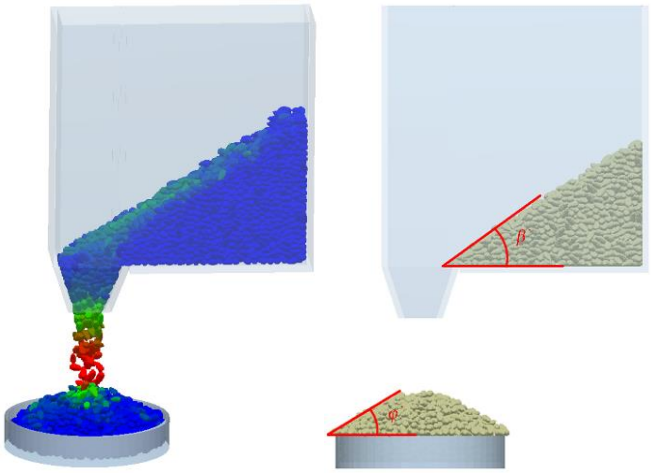

Fig. 5 - Simulated seed dropping test

The Plackett-Burman experiment was designed in Design-Expert V8.0 (Stat-Ease) and the repose and accumulation angles of the cotton population were used as the response values to identify the simulation parameters with a significant influence on the response value. A total of 8 (X_1-X_8) parameters were calibrated in the simulation test, as well as 3 virtual parameters (X_9-X_{11}).

In particular, parameters X_1-X_8 represent the high and low levels of each parameter in the form of 1 0, and - 1, are selected. A total of 12 simulation test groups were performed. Based on extensive preliminary testing and related references, 8 cotton seed simulation parameters were selected. Table 1 reports the ranges of the parameters that were calibrated.

Table 1

Parameters used in the Plackett Burman tests

Symbol	Parameter	Level		
		-1	0	1
X_1	Poisson's ratio	0.10	0.30	0.50
X_2	Shear modulus/MPa	5	9	14
X_3	Collision recovery coefficient between cotton-seed and plexiglass	0.10	0.40	0.70
X_4	Static friction coefficient between cotton-seed and plexiglass	0.30	0.50	0.70
X_5	Dynamic friction coefficient between cotton-seed and plexiglass	0.15	0.25	0.35
X_6	Collision recovery coefficient between cotton-seeds	0.20	0.40	0.60
X_7	Static friction coefficient between cotton-seeds	0.10	0.30	0.50
X_8	Dynamic friction coefficient between cotton-seeds	0.01	0.09	0.17
X_9、X_{10}、X_{11}	Virtual parameters			

Table 2 reports the design scheme and simulation results of the Plackett-Burman screening test. Design-Expert was used to analyse the variance of the simulation test results in order to obtain the influence of each calibration parameter on the simulation (Table 3). Static friction coefficient between cotton-seeds (SFCC) and dynamic friction coefficient between cotton-seeds (DFCC) are the only parameters observed to have a significant effect on the repose and accumulation angles. These two parameters were thus selected for optimization in the steepest climb and the CCD tests.

Table 2

Design scheme and results of the Plackett Burman test

No.	X_1	X_2	X_3	X_4	X_5	X_6	X_7	X_8	X_9	X_{10}	X_{11}	Repose angle / °	Accumulation angle / °
1	1	-1	-1	1	-1	-1	-1	1	-1	1	-1	29.16	22.64
2	1	1	1	-1	1	-1	-1	-1	-1	-1	1	21.18	17.62
3	-1	-1	1	1	-1	1	-1	-1	-1	-1	-1	21.08	16.27
4	1	1	-1	1	1	-1	1	-1	1	-1	-1	40.66	34.34
5	1	-1	1	-1	1	1	-1	1	1	1	-1	29.11	22.28
6	1	-1	1	1	-1	1	1	-1	1	1	1	39.06	35.55
7	-1	1	1	1	1	-1	1	1	-1	1	1	61.09	42.14
8	-1	1	-1	1	1	1	-1	1	1	-1	1	30.32	26.02
9	-1	1	-1	-1	1	1	1	-1	1	1	-1	30.90	26.80
10	1	-1	-1	-1	-1	1	1	1	-1	1	1	51.72	40.95
11	-1	1	1	-1	-1	-1	1	1	1	-1	1	52.87	44.22
12	-1	-1	-1	-1	-1	-1	-1	-1	-1	-1	-1	18.63	17.86

Table 3

Significance analysis of the Plackett-Burman test parameters

Parameter	Repose angle				Accumulation angle			
	df	Sum of square	F-value	P-value	df	Sum of square	F-value	P-value
X_1	1	3.97	0.19	0.6941	1	1.76	0.14	0.7358
X_2	1	3.32	0.16	0.7186	1	5.16	0.40	0.5710
X_3	1	44.09	2.08	0.2447	1	7.47	0.58	0.5013
X_4	1	23.98	1.13	0.3653	1	4.35	0.34	0.6013
X_5	1	2.60	0.12	0.7494	1	10.49	0.82	0.4327
X_6	1	37.17	1.76	0.2771	1	1.62	0.13	0.7463
X_7	1	957.47	45.22	0.0067**	1	509.29	39.66	0.0081**
X_8	1	570.59	26.95	0.0139*	1	206.83	16.11	0.0278*

*Note:** and * indicate significance at P < 0.01 and P < 0.05, respectively.*

Following the Plackett-Burman screening test results, the relative errors of the repose angle (RERA) and the relative errors of the accumulation angle (REAA) were taken as the objectives. Moreover, during the simulation tests, SFCC X_7 and DFCC X_8 were gradually increased based on a predetermined step size, while the remaining parameters were set as intermediate values.

RERA Y_1 and REAA Y_2 were obtained as follows:

$$Y_1 = \frac{|\beta_0 - \beta'|}{\beta_0} \times 100\% \quad (2)$$

$$Y_2 = \frac{|\varphi_0 - \varphi'|}{\varphi_0} \times 100\% \quad (3)$$

Figure 6 presents the experimental scheme and results of the steepest ascent experiment. The RERA and REAA are observed to initially decrease and subsequently increase with increasing SFCC X_7 and DFCC X_8, respectively. The RERA and REAA values determined in the test, when the SFCC and DFCC were 0.2 and 0.05 respectively, exhibit the lowest relative errors. Thus, test was selected as the central point and set as the medium level, while tests 1 and 3 were set as the low and high levels, respectively for the CCD simulation test.

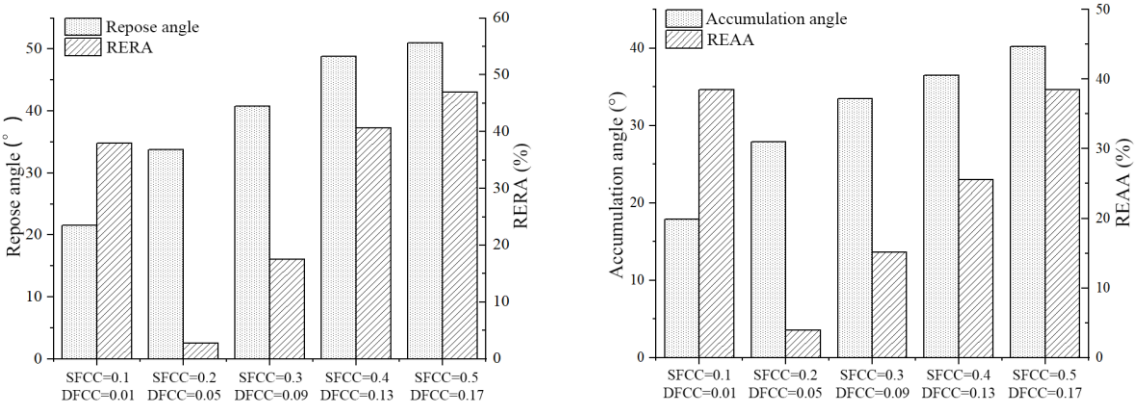

(a) (b)

Fig. 6 - Design scheme and results of the steepest ascent experiment under different parameters.
(a) Repose angle and RERA; (b) Accumulation angle and REAA.

Table 4

Simulation test factor code

Code	SFCC X_7	DFCC X_8
-1.4142	0.1	0.01
-1	0.13	0.02
0	0.2	0.05
1	0.27	0.08
1.4142	0.3	0.09

The results of the steepest climbing test (Figure 8) determined SFCC X_7 and DFCC X_8 as the experimental factors for the CCD, and RERA and REAA as the experimental indexes. Table 4 presents the test factor coding. A total of 13 tests were performed, with the details reported in Table 5.

Table 5

Design scheme and results of the central composite test

Test No.	X_7	X_8	Repose angle/°	RERA/%	Accumulation angle /°	REAA/%
1	1(0.27)	1(0.08)	37.66	8.53	31.44	8.23
2	1.414(0.3)	0(0.05)	38.29	10.36	31.75	9.32
3	1	-1	37.34	7.61	30.60	5.36
4	0(0.2)	0	35.22	1.52	29.77	2.51
5	0	1.414(0.09)	36.02	3.81	29.74	2.38
6	0	0	35.45	2.16	29.41	1.24
7	0	0	35.14	1.28	28.22	2.85
8	-1(0.13)	-1(0.02)	31.90	8.07	26.77	7.84
9	-1.414(0.1)	0	32.79	5.48	27.50	5.32
10	0	-1.414(0.01)	33.00	4.88	27.92	3.89
11	-1	1	33.72	2.82	28.40	2.24
12	0	0	33.81	2.56	28.50	1.89
13	0	0	34.17	1.53	28.41	2.18

Note: Bracketed numbers denote the test factor level values

Thus far, we selected RERA Y_1 and REAA Y_2 as the response values, and SFCC X_7 and DFCC X_8 as the variables, resulting in a multi-objective constrained optimization problem. In contrast to single-objective optimization problems, multi-objective optimization problems do not have a unique solution, but rather an optimal solution set denoted as the Pareto optimal solution. The NSGA-Ⅱ genetic algorithm is a popular multi-objective genetic algorithm (GA) that employs a fast non-inferior hierarchical sorting mechanism. Its advantages include a fast running speed and the ability to accurately approximate the Pareto optimal solution. Furthermore, by introducing the congestion degree and congestion degree comparison operator, the uniformity of the Pareto optimal solution dispersion is guaranteed. In this paper, the GA Pareto score, initial population size and genetic algebra were set to 0.3, 200, and 600, respectively.

RESULTS AND DISCUSSION

Multiple regression fitting was performed based on the test results and the test data (Table 5). The regression models of the effect of SFCC X_7 and DFCC X_8 on RERA Y_1 and REAA Y_2 are described as follows:

$$Y_1=36.50-277.17X_7-329.45X_8+734.52X_7X_8+655.36X_7^2+1581.94X_8^2 \quad (4)$$

$$Y_2=35.20-262.40X_7-301.24X_8+853.57X_7X_8+587.09X_7^2+1038.06X_8^2 \quad (5)$$

Table 6 reports the significance test results of the regression models. The fitting degrees of both models are observed to be highly significant ($P < 0.01$). The first term (X_8) of DFCC exerts a significant effect on RERA ($P < 0.05$), while the other terms have a highly significant effect on RERA ($P < 0.01$). The first (X_8) and quadratic (X_8^2) terms of DFCC X8 have a significant effect on REAA ($P < 0.05$), while the remaining terms have a highly significant effect on REAA ($P < 0.01$). This indicates that the primary, interaction and quadratic terms of SFCC X_7 and DFCC X_8 exert a significant influence on RERA and REAA. Furthermore, a quadratic relationship is identified by the influence of test factors on the response value. The *P*-values of the loss fitting item are determined as 0.2197 and 0.3690 for RERA and REAA respectively, revealing the lack of significance between these two variables. This demonstrates that there are no other factors affecting the indicators for both models. The goodness of fit (R^2) of the two regression equations were determined as 0.95 and 0.97, respectively. This indicates the strong fit between the predicted and actual values and the ability of the independent variable to explain the dependent variable to a higher degree.

Table 6

Regression analysis of variance for models RERA and REAA

Source	RERA				REAA			
	Sum of square	df	F-value	P-value	Sum of square	df	F-value	P-value
Model	111.12	5	47.98	< 0.0001**	85.29	5	38.68	< 0.0001**
X_7	18.46	1	39.85	0.0004**	10.50	1	23.82	0.0018**
X_8	4.27	1	9.21	0.0190*	2.96	1	6.71	0.0359*
$X_7 X_8$	9.52	1	20.55	0.0027**	17.94	1	40.66	0.0004**
X_7^2	71.74	1	154.88	< 0.0001**	53.20	1	120.63	< 0.0001**
X_8^2	14.10	1	30.44	0.0009**	3.15	1	7.14	0.0319*
Residual	3.24	7			3.09	7		
Lack of fit	2.11	3	2.50	0.2197	1.57	3	1.38	0.3690
Pure Error	1.13	4			1.51	4		
Cor Total	114.37	12			88.38	12		

*Note: ** and * indicate significance at P < 0.01 and P < 0.05, respectively*

The experimental data was then processed by Design-Expert V8.0 to determine the response surface of the effect of SFCC X_7 and DFCC X_8 on RERA Y_1 and REAA Y_2. Figure 7 presents the interaction effect between the two influence parameters via the response surface. Stronger effects of SFCC X_7 and DFCC X_8 resulted in an initial decrease and subsequent decrease in the RERA Y_1 of the REAA Y_2. In addition, SFCC X_7 and DFCC X_8 values between 0.15-0.23 and 0.04-0.07 resulted in relatively small values of RERA and REAA.

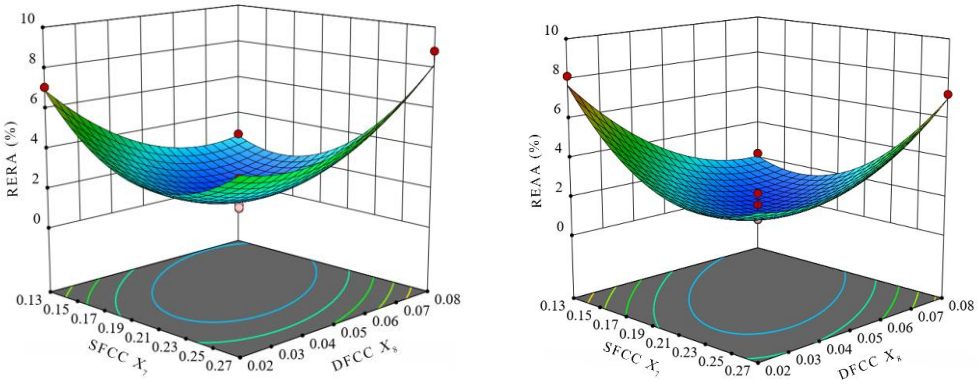

Fig. 7 - Influence of interaction between SFCC and DFCC on RERA and REAA

(a) Influence of interaction between SFCC and DFCC on RERA; (b) Influence of interaction between SFCC and DFCC on REAA

In order to minimize RERA and REAA, SFCC and DFCC were taken as the optimization objects based on the climbing test results (Table 3), with values of 0.1-0.3 and 0.01-0.09, respectively. The objective and constraint functions of the final optimization problem are described as follows:

$$\begin{cases} \min(Y_1(X_7, X_8), Y_2(X_7, X_8)) \\ \text{s.t.} \begin{cases} 0.1 \le X_7 \le 0.3 \\ 0.01 \le X_8 \le 0.09 \end{cases} \end{cases} \quad (6)$$

Figure 8 presents the Pareto optimal solution set obtained by NSGA - II. It is impossible to simultaneously achieve the optimal solution for each objective under the multi-objective optimization problem. Therefore, REAA increases as RERA is reduced. Under the condition of two objectives, SFCC is determined as 0.174 and DFCC as 0.068, with RERA and REAA as 1.715% and 1.712%, respectively.

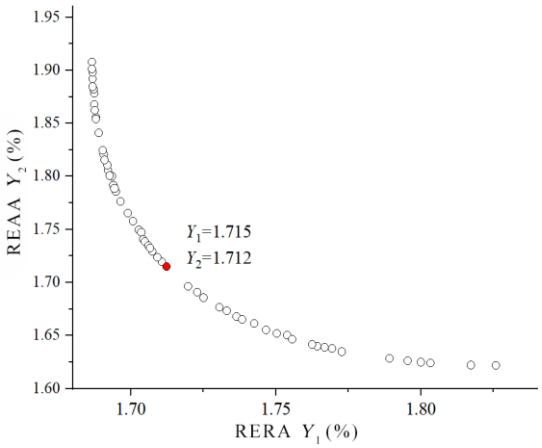

Fig. 8 - Pareto optimal solution set curve, the red data point is the optimal solution

We then verified that the optimal parameters satisfy the test results. SFCC and DFCC were set as 0.174 and 0.068, respectively and the other non-significant parameters were taken as intermediate levels. Poisson's ratio, the shear model, and the recovery coefficient of collision between cotton-seeds were set as 0.3, 9 MPa and 0.4, while the recovery, friction and dynamic friction coefficients of cotton-seed and plexiglass were set as 0.4, 0.5 and 0.25, respectively. These parameters were imported into EDEM for the simulations in order to obtain the contour comparison of the repose and accumulation angles between the simulation and actual tests (Figures 9 and 10, respectively). The contour lines of the simulation and actual tests are in agreement. The average repose and accumulation angles were determined as 34.07° and 28.55°, respectively. The T-test results of the test samples determined P-values of 0.5516 and 0.7432 for the repose and accumulation angles respectively, both of which are greater than 0.05. Furthermore, the results demonstrate that the repose and accumulation angles derived via the simulation are not significantly different to the actual physical test values.

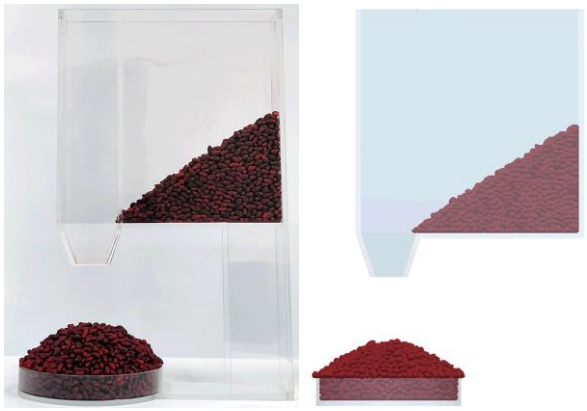

(a) (b)

Fig. 9 - Experimental results

(a) Physical experiment; (b) Simulation experiment

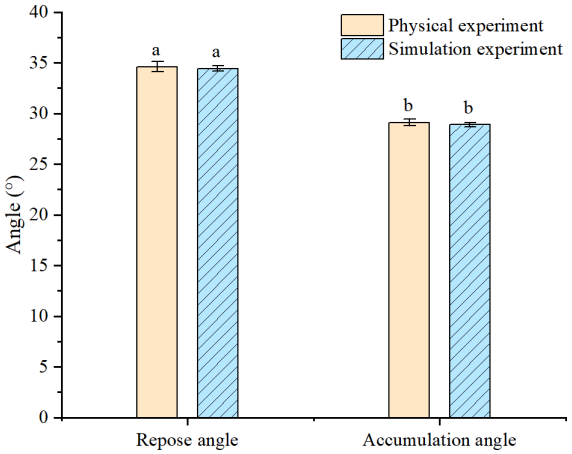

Fig. 10 - Verification of discrete element simulation

CONCLUSIONS

A device was designed to obtain the repose and accumulation angles of particle materials. The actual repose and accumulation angles of the Zhongmian-96A coated cotton seed were measured as 34.70° and 29.05°, respectively. A Plackett-Burman screening test was carried out with the repose and accumulation angles as the test indexes. The parameters SFCC and DFCC were observed to have a significant influence on the index. The CCD was then adopted by taking these two parameters as the experimental factors and RERA and REAA as the indicators. Analysis of variance revealed the first, interaction and quadratic terms of the two test parameters to have significant effects on RERA and REAA ($P < 0.05$). Multiple regression fitting of the test data was applied to determine the regression equation of the two indexes, with goodness of fit (R^2) values of 0.95 and 0.97, respectively. This reveals the strong fitting degree for both equations. The minimum values of RERA and REAA were taken as the optimization objectives, and SFCC and DFCC as the optimization objects. The NSGA - Ⅱ genetic algorithm was employed to solve the multi-objective optimization of the mathematical model, outputting the Pareto optimal solution set. Considering the two optimization objectives, SFCC, DFCC, RERA and REAA were determined as 0.174, 0.068, 1.715% and 1.712%, respectively. A simulation test was performed to verify the test results based on the parameters of the optimal solution. The results demonstrate that there are no significant differences between the repose and accumulation angles of the simulation and physical test results, indicating the high reliability of the optimal combination of the discrete element simulation parameters.

It should be noted that the DEM parameters of coated cotton seeds obtained in this study were calibrated for specific moisture content and under laboratory conditions. In further research, the relationship between DEM parameters of coated cotton seed and moisture content should be established, the contact parameters of cotton seed and different materials should be researched, and the influence of agricultural granule materials under actual working conditions should be considered. By exploring the contact behaviour between particle flow and mechanical parts, the DEM input parameters calibrated in this study can provide a reference for the design and development of cotton seeder.

ACKNOWLEDGEMENT

This research was supported by the National Natural Science Foundation of China funded by the Chinese government (11562019); and the President fund by the Tarim University (TDZKQN201803).

REFERENCES

[1] Baryeh, E., Mangope, B. (2003). Some physical properties of QP-38 variety pigeon pea. *Journal of Food Engineering*, 56: 59-65.

[2] Binelo, M., Delima, R., Khatchatourian, O., et al, (2019). Modelling of the drag force of agricultural seeds applied to the discrete element method. *Biosystems Engineering*, 178: 168-175.

[3] Furuhata, M., Ohsumi, A., & Chosa, T. (2011). Hardness, colour and germination characteristics of rice seed iron-coated to avoid bird damage-seed pretreatment, type and amount of coating material. *Japanese Journal of Crop Science*, 80: 302-311.

[4] Gao, X., Zhou, Z., Xu, Y., et al, (2020). Numerical simulation of particle motion characteristics in quantitative seed feeding system. *Powder Technology*, 367, 643-658.
[5] Ghodki, B., Patel, M., Namdeo, R., et al, (2019). Calibration of discrete element model parameters: soybeans. *Computational Particle Mechanics*, 6: 3-10.
[6] Han, D., Zhang, D., Jing, H., et al, (2018). DEM-CFD coupling simulation and optimization of an inside-filling air-blowing maize precision seed-metering device. *Computers and Electronics in Agriculture*, 150: 426-438.
[7] Hou, Junming, Zhu, Hongjie, Li, J., et al, (2020). Analysis and optimization on the process of adjustable double drum castor shelling based on discrete element method. *INMATEH-Agricultural Engineering*, 62(3), 289-298.
[8] Li, X., Yan, Q., Li, C., et al, (2018). Seed coating on cotton seedling cold tolerance control and screening of cold resistant seed coating agent. （种衣剂对棉花幼苗耐寒性的观测及耐寒种衣剂筛选）*Journal of China Agricultural University*, 23: 38-47.
[9] Liang, R., Chen, X., Jiang, P., et al, (2020). Calibration of the simulation parameters of the particulate materials in film mixed materials. International *Journal of Agricultural and Biological Engineering*, 13: 29-36.
[10] Liu, F., Zhang, J., Li, B., et al, (2016). Calibration of parameters of wheat required in discrete element method simulation based on repose angle of particle heap. （基于堆积试验的小麦离散元参数分析及标定）*Transactions of the Chinese Society of Agricultural Engineering*, 32: 247-253.
[11] Qi, X., Hu, T., Wang, Y., et al, (2019). Physical characteristics analysis and discrete element modelling of carrot seeds. *International Agricultural Engineering Journal*, 28: 236-243.
[12] Wang, S., Hu, J., Ji, J., et al, (2020). Experimental Study and Computer Simulation of Compression Characteristics and Crushing of Chinese Cabbage Seeds. *Applied Engineering in Agriculture*, 36: 815-828.
[13] Xue, P., Xia, X., Gao, P., et al, (2019). Double-setting seed-metering device for precision planting of soybean at high speeds. *Transactions of the ASABE*, 62: 187-196.
[14] Yan, D., Yu, J., Wang, Y., et al, (2020). A general modelling method for soybean seeds based on the discrete element method. *Powder Technology*, 372: 212-226.
[15] Zhang, H., Li, Y., Xu, C., et al, (2020). Optimization research of fertilizer guiding mechanism based on the discrete element method. *INMATEH-Agricultural Engineering*, 60(1), 275-286. doi:10.35633/inmateh-60-31
[16] Zhou, L., Yu, J., Wang, Y., et al, (2020). A study on the modelling method of maize-seed particles based on the discrete element method. *Powder Technology*, 374: 353-376.